

# We are IntechOpen, the world's leading publisher of Open Access books Built by scientists, for scientists

6,900

Open access books available

186,000

International authors and editors

200M

Downloads

Our authors are among the

154

Countries delivered to

TOP 1%

most cited scientists

12.2%

Contributors from top 500 universities



WEB OF SCIENCE™

Selection of our books indexed in the Book Citation Index  
in Web of Science™ Core Collection (BKCI)

Interested in publishing with us?  
Contact [book.department@intechopen.com](mailto:book.department@intechopen.com)

Numbers displayed above are based on latest data collected.  
For more information visit [www.intechopen.com](http://www.intechopen.com)



# Efficient Computational Techniques in Bioimpedance Spectroscopy

Aleksander Paterno, Lucas Hermann Negri and Pedro Bertemes-Filho  
*Department of Electrical Engineering, Center of Technological Sciences  
Santa Catarina State University, Joinville,  
Brazil*

## 1. Introduction

Electrical Bioimpedance Analysis (BIA) is an important tool in the characterization of organic and biological material. For instance, its use may be mainly observed in the characterization of biological tissues in medical diagnosis (Brown, 2003), in the evaluation of organic and biological material suspensions in biophysics (Cole, 1968; Grimnes & Martinsen, 2008), in the determination of fat-water content in the body (Kyle et al., 2004) and in *in vivo* identification of cancerous tissues (Aberg et al., 2004), to name a few important works. It is also natural to have different computational approaches to bioimpedance systems since more complex computational techniques are required to reconstruct images in electrical impedance tomography (Holder, 2004), and this would open a myriad of other computational and mathematical questions based on inverse reconstruction problems.

In many practical cases, the obtained bioimpedance spectrum requires that the produced signal be computationally processed to guarantee the quality of the information contained in it, or to extract the information in a more convenient way. Such algorithms would allow the removal of redundant data or even the suppression of invalid data caused by artifacts in the data acquisition process. Many of the discussed computational methods are also applied in other areas that use electrical impedance spectroscopy, as in chemistry, materials sciences and biomedical engineering (Barsoukov & Macdonald, 2005).

BIA systems allow the measurement of an unknown impedance across a predetermined frequency interval. In a typical BIA system, the organic or biological material suspension or tissue sample to be characterized is excited by a constant amplitude sine voltage or current and the impedance is calculated at each frequency after the other parameter, current or voltage, is measured. This technique is called sine-correlation response analysis and can provide a high degree of accuracy in the determination of impedances. By using the sine-correlation technique, the spectrum is determined either by obtaining the impedance real and imaginary parts, or by directly obtaining its modulus and phase. For this purpose, analog precision amplifiers and phase detectors provide signals proportional to modulus and phase at each frequency, and the interrogated frequency range is usually between 100 Hz up to 10 MHz. In such BIA systems the current signal used in the sample excitation is band-limited, because the output impedance of the current source and the open-loop gain of its amplifiers are low, especially at high frequencies (Bertemes-Filho, 2002). Some of these limitations may be

avoided by using digital signal processing techniques that may take the place of the electronic circuitry that have frequency constraints.

In the BIA electronics, when considering the phase detection part of analog circuits used, a high-precision analog multiplier provides a constant signal proportional to the phase of its input. However, the frequency response of the circuit is usually limited, for example, to 1 MHz and such multipliers require the excitation source signal as a reference. A software solution would provide an alternative to the use of such phase detectors, where in some cases an algorithm may be capable of calculating the phase spectrum from the acquired modulus values. With this system configuration, phase/modulus retrieval algorithms may be used to obtain the phase or modulus of an impedance, considering that one of these sets of values has been electronically obtained.

In electrical bioimpedance spectroscopy applied to medical diagnosis, research groups cite the use of the Kramers-Kronig causality relations Kronig (1929) to obtain the imaginary part from the real part (or equivalently phase/modulus from modulus/phase parts) of a causal spectrum (Brown, 2003; Nordbotten et al., 2011; Riu & Lapaz, 1999; Waterworth, 2000). A similar procedure occurs when obtaining the modulus from the phase, or vice-versa, using the Hilbert transform in a causal signal (Hayes et al., 1980). With constraints on the characteristics of the acquired phase or modulus spectrum, the use of these algorithms may allow the calculation of the missing part of an electrical bioimpedance spectrum. In addition, such algorithms may be used to validate the obtained experimental impedance spectrum (Riu & Lapaz, 1999). However, there may be restrictions to the signals that can be processed with these techniques, specifically with the Fourier-transform based phase/modulus-retrieval algorithms (Paterno et al., 2009), even though it may provide a computationally efficient solution to the problem.

Still related to the multi-frequency BIA systems, after the raw non-processed information is acquired, the choice of an appropriate numerical model function to fit the experimental data and generate a summary of the information in the spectrum condensed in a few parameters is also another niche where computational techniques may be used. The choice of an efficient fitting method to be used with experimental data and with a non-linear function, as the Cole-Cole function, is a problem that has been previously discussed in the literature (Halter et al., 2008; Kun et al., 2003; 1999). It is natural to think that once such algorithms work for the fitting with a non-linear Cole-Cole function, they will also work with other different non-linear functions in bioimpedance experimental data. With this in focus, an algorithm is demonstrated that shows novelties in terms of computational performance while fitting experimental data using the Cole-Cole function as part of the fitness function and particle-swarm optimization techniques to optimally adjust the model function parameters (Negri et al., 2010). Other computational intelligence algorithms are also used for comparison purposes and a methodology to evaluate the results of the fitting algorithms is proposed that uses a neural network.

The experimental data in this work were obtained with a custom-made multi-frequency bioimpedance spectrometer (Bertemes-Filho et al., 2009; Stiz et al., 2009). Samples of biological materials were used like bovine flesh tissue and also raw milk, that may constitute a suspension of cells, since the samples of raw milk may have cells, for example, due to mastitis infection in sick animals. Other characteristics of milk, which are currently important in the dairy industry, could be evaluated, as, for instance, a change in the water content or even the

presence of an illegal adulterant, like hydrogen peroxide (Belloque et al., 2008). The problem was then to characterize the raw milk with such adulterants using the bioimpedance spectrum either fitted to a Cole-Cole function or not (Bertemes-Filho, Valicheski, Pereira & Paterno, 2010). The neural network algorithm may be in this particular case a useful technique to classify the milk with hydrogen peroxide (Bertemes-Filho, Negri & Paterno, 2010).

As a summary, the authors provided a compilation of problems into which computational intelligence and digital signal processing techniques may be used, as well as the illustration of new methodologies to evaluate the processed data and consequently the proposed computational techniques in bioimpedance spectroscopy.

## 2. Materials and methods

### 2.1 The BIA system to interrogate bioimpedances

The used BIA system is based on a bioimpedance spectrometer consisting of a current source that injects a variable frequency signal into a load by means of two electrodes. It then measures the resulting potential in the biological material sample with two other electrodes and calculates the transfer impedance of the sample. The complete block diagram of the spectrometer system is shown in fig. 1. A waveform generator (FGEN) board supplies a sinusoidal signal with amplitude of  $1 V_{pp}$  (peak-to-peak) in the frequency range of 100 Hz to 1 MHz. The input voltage ( $V_{input}$ ) is converted to a current ( $+I$  and  $-I$ ) by a modified bipolar Howland current source (also known as voltage controlled current source) (Stiz et al., 2009), which injects an output current of  $1 mA_{pp}$  by two electrodes to the biological material under study. The resulting voltage is measured with a differential circuit between the other two electrodes by using a wide bandwidth instrumentation amplifier (Inst. Amp. 02). The amplitude of the injecting current is measured by another instrumentation amplifier (Inst. Amp. 01) while using a precision shunt resistor ( $R_{shunt}$ ) of  $100 \Omega$ . A custom made tetrapolar impedance probe was used to measure the bioimpedance and is composed of 4 triaxial cables. The outer and inner shields of the cables are connected together to the ground of the instrumentation. The tip of the probe has a diameter of 8 mm (D), and the electrode material is a wire of 9 carat gold with a diameter of 1 mm (d). The wires are disposed in a circular formation about the longitudinal axis. Finally, a data acquisition (DAQ) board measures both voltage load and output current by sampling the signals at a maximum sampling frequency of 1.25 MSamples/s for each of the possible 33 frequencies in the range. Data are stored in the computer for the processing of the bioimpedance spectra. Although the modulus and phase of the load are electronically obtained, one of the parameters can be used to experimentally validate the phase/modulus retrieval technique while comparing the calculated and measured values.

For completeness purposes, if one decides to use the bioimpedance spectrum points at frequencies which were not used in the excitation or were not acquired, the value at this frequency can be determined by means of interpolation, since the evaluated spectra are usually well-behaved.

The nature of the experimental bioimpedance spectra is important for the use of the algorithms described in this work. It is assumed here that the experimental sample bioimpedance spectrum may have its points represented by a Cole-Cole function in the interrogated frequency range. This is a plausible supposition, since it is a function that represents well many types of bioimpedance spectra associated with cell suspensions and

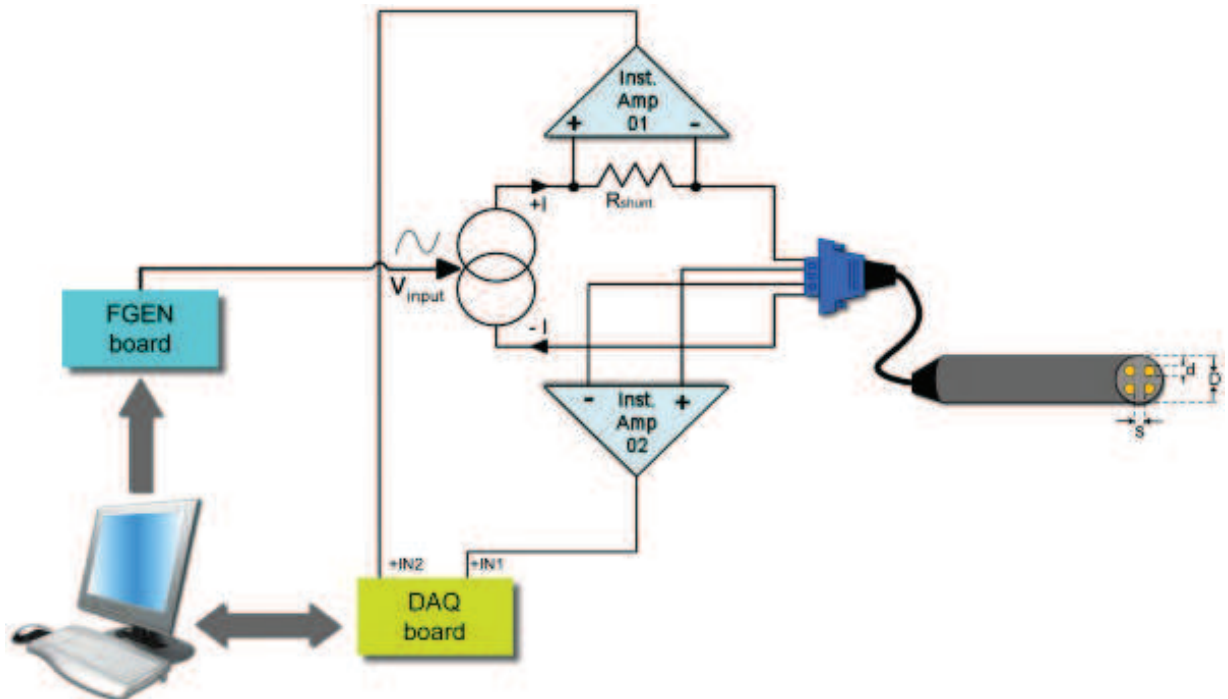


Fig. 1. BIA system complete block diagram for the interrogation of electrical bioimpedances.

many types of organic tissues and materials (Cole, 1940; 1968; Grimnes & Martinsen, 2008). When the Cole-Cole function shown in the following equations is not an appropriate model function to fit the experimental data, the data are not processed with these algorithms and are used in phase/modulus retrieval or in the neural network without further processing.

## 2.2 Cole-Cole fractional order impedance function

Tissues or non-uniform cell suspensions have bioimpedance spectra that are not well represented by a Debye-type single-pole (single-relaxation) function. In any case, the bioimpedance may be represented as a complex number in polar or cartesian, as in eq. 1:

$$Z(s) = |Z(s)|e^{j\theta} = Z_R(s) + jZ_I(s) \quad (1)$$

where  $s = j\omega$ ,  $\omega$  represents the angular frequency and  $j = \sqrt{-1}$ . The cartesian form takes its graphical representation in the complex impedance plane where the ordinate axis is the negative of the impedance imaginary part (-reactance) and the abscissa axis is the real part of the impedance. Usually different configurations of a semi-circular arc in the complex impedance plane may represent the experimental bioimpedances spectra or they may be depicted by plotting the modulus and phase versus frequency.

In addition, the bioimpedance function used in this work is going to be represented within a limited frequency range in terms of a distribution function of relaxation times,  $\tau$ , which would correspond to the spectrum of cell sizes, particles or molecules in a suspension or tissue. This distribution function approach was proposed by Fuoss and Kirkwood (Fuoss & Kirkwood, 1941) where they extended the Debye theory from which a relation can be obtained between the distribution function,  $G(\tau)$ , and a transfer function,  $Z(s)$ , that corresponds in this case to

a bioimpedance. This relation is given by:

$$Z(s) = \int_0^{\infty} \frac{G(\tau)}{1 + s\tau} d\tau \quad (2)$$

By using eq.2, the relation between  $Z(s)$  and  $G(\tau)$  is stressed:

$$Z_{frac}(s) = \frac{R_0 - R_{\infty}}{1 + (s\tau_0)^{\alpha}} = (R_0 - R_{\infty}) \int_0^{\infty} \frac{G(\tau)}{1 + s\tau} d\tau \quad (3)$$

In eq. 3, the frequency dependent part of the impedance in the Cole-Cole type model function,  $Z_{frac}(s)$ , is represented, where  $R_0$  is the impedance resistance at very low frequencies,  $R_{\infty}$  is the resistance at very high frequencies, and the function containing the fractional order term,  $(s\tau_0)^{\alpha}$  can be represented by an integral of the distribution function  $G(\tau)$  (Cole & Cole, 1941), and  $\alpha$  is a constant in the interval  $[0, 1]$  and  $\tau_0$  is the generalized relaxation time.  $G(\tau)$  is a distribution function for the fractional order Cole-Cole model function and is explicitly represented by Cole & Cole (1941):

$$G(\tau) = \frac{1}{2\pi} \left[ \frac{\sin [(1 - \alpha)\pi]}{\cosh \left[ \alpha \log \left( \frac{\tau}{\tau_0} \right) \right] - \cos [(1 - \alpha)\pi]} \right] \quad (4)$$

The complete model developed by Cole and Cole consists of an equation, an equivalent circuit and a complex impedance circular arc locus, and in terms of impedances, after integrating eq. 3, one obtains the Cole-Cole function to represent the evaluated impedance spectrum:

$$Z_{Cole}(\omega) = R_{\infty} + \frac{R_0 - R_{\infty}}{1 + (j\omega\tau_0)^{\alpha}} \quad (5)$$

In eq. 5, the variable  $Z_{Cole}(\omega)$  is a complex impedance and is a function of the angular frequency  $\omega$ . The Cole-Cole function was obtained by the Cole and Cole brothers when they also introduced the distribution function of eq. (4). It is worth noticing that the function containing the fractional order term,  $(s\tau_0)^{1-\alpha}$  instead of the  $(s\tau_0)^{\alpha}$ , was originally used in a model for dielectrics (Cole & Cole, 1941).

For the use of the phase/modulus retrieval algorithm in  $Z_{Cole}(s)$  the independent term corresponding to the resistance,  $R_{\infty}$ , causes the frequency dependent function to satisfy neither the phase- nor the modulus-retrieval algorithm conditions (Hayes et al., 1980; Paterno et al., 2009). In other words, the experimental points to be used with the phase/modulus retrieval algorithm must be previously tested with known bioimpedance spectrum data to verify if the process is applicable. Consequently, the algorithm has limitations of use if the resistance at very high frequencies is not zero, or if the condition of minimum phase in the spectrum is not satisfied. In addition to that, for the reconstruction of phase and modulus of  $Z_{Cole}(s)$ , the experimental data must correspond to a Cole-Cole spectrum that may be fitted to a specific set of values of  $\alpha$  (Paterno et al., 2009), otherwise the algorithm may not converge to the correct values. Fortunately, these values of  $\alpha$  with which the algorithm properly works correspond to a broad class of tissues, cell suspensions and organic materials to be evaluated in practical cases. In the limit, when  $\alpha \approx 0$ ,  $Z_{frac}(s)$  becomes a pure resistance having minimum-phase. For values of  $\alpha$  in the interval  $(0, 1)$ , the modulus retrieval algorithm may be capable of producing a limited error, as demonstrated elsewhere (Paterno et al.,

2009). For the use of instrumentation to characterize the spectrum of organic material, these conditions are usually met, as in the illustrative case of bioimpedances obtained from mango, banana, potato and guava, shown in the results in section 3. These are illustrative examples of organic material to have its impedance phase measured and used as input to the algorithm that determines the bioimpedance modulus. In this case, both parameters were measured to validate the results (Paterno & Hoffmann, 2008).

### 2.3 Phase/modulus retrieval algorithm description

The algorithm is based on the flowchart in fig. 2. It starts by being fed with the modulus sequence vector (in the phase retrieval algorithm) provided by electronic means. In the case of using the modulus retrieval procedure, phase and modulus must be interchanged in the algorithm. A vector containing the  $N$  modulus samples equally spaced in frequency is saved in  $|Z_{OR}(k)|$  and a vector that contains the estimated phase samples is initialized with random values. The initial impedance Fourier transform spectrum is a vector represented by the  $N$  values,  $Z_{OR}(k) = |Z_{OR}(k)|e^{j\theta_{est}}$ . In the following step, the real part of an  $M$ -point inverse fast-Fourier transform (IFFT) algorithm is used to produce a sequence in the time-domain,  $z_{est}[n]$ . An  $M$ -point IFFT is used, where the constraint  $M \geq 2N$  guarantees the algorithm convergence. Only the real part of the  $M$ -point IFFT is used because the input signal is real in the time-domain (Quartieri & Oppenheim (1981), and has an even Fourier transform, allowing half of the samples ( $N$  samples) to represent the bioimpedance spectrum.

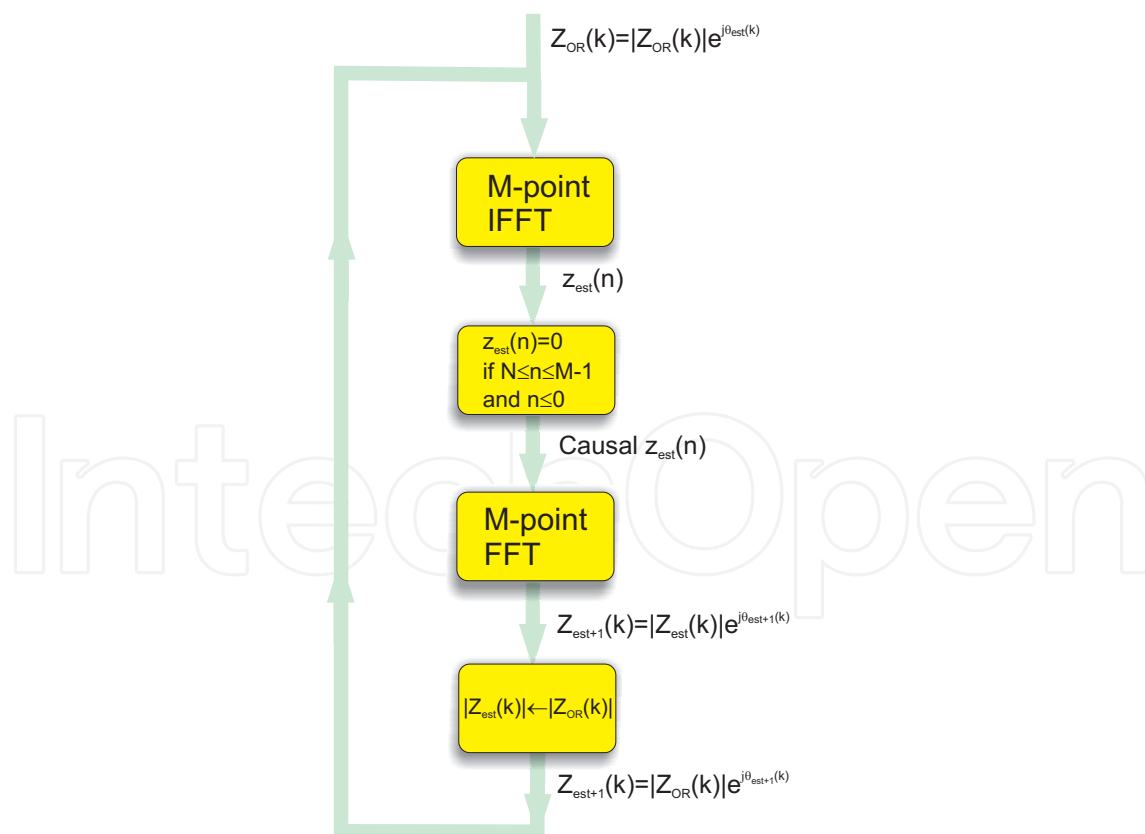


Fig. 2. Flowchart representing the processing steps in the modulus-retrieval algorithm for the BIA system.

Causality is imposed in the fourth block while a finite length constraint on the time-domain sequence sets  $z_{est}(n)$  to zero for  $n > N - 1$ . The  $M$ -point FFT of the data set containing  $z(n)$  produces the estimates of the bioimpedance spectrum. This flowchart indicates the process that is repeated until the root-mean squared value of the difference between two consecutive estimated vectors is less than a stopping parameter,  $\epsilon$ . It was set equal to  $\epsilon = 10^{-6}$ , which is a much lower value than the necessary modulus or phase resolution in BIA systems. The length of the input vector sequences is a power of 2, since the iterative solution uses uniformly spaced samples Quartieri & Oppenheim (1981) and the Fast-Fourier Transform (FFT) radix-2 algorithm (Proakis & Manolakis, 2006).

## 2.4 Computational intelligence algorithms in electrical bioimpedance spectroscopy

In this section computational intelligence algorithms will be briefly described such as to be used in an application to fit experimental data obtained with BIA systems using particle swarm optimization techniques; additionally, artificial neural networks (ANN) are described to provide a methodology to evaluate the fitting algorithms. The performance testing is implemented by associating the training phase of the ANN to previously known information contained in the bioimpedance spectrum. For example, in the evaluated sample. The presence of different adulterants in raw milk, specifically water and hydrogen peroxide, and the characterization of the type of bovine flesh tissue are samples that were interrogated with the BIA system. The ANN is used to evaluate how much information the fitting process may extract from the experimental data such as to condense it into the parameters of the used function model, namely, the Cole-Cole function that contains four parameters ( $R_0$ ,  $R_\infty$ ,  $\tau$  and  $\alpha$ ) as in eq.5 with the information of the electrical bioimpedance spectrum.

### 2.4.1 The Particle-Swarm Optimization (PSO) experiment

The particle swarm optimization algorithm was used to extract the Cole-Cole function parameters,  $R_0$ ,  $R_\infty$ ,  $\tau_0$  and  $\alpha$  from experimental data. For this experiment, the previously described bioimpedance spectrometer injected a sinusoidal current via the two electrodes of a tetrapolar probe into bovine liver, heart, topside, and back muscle samples. A cow was killed in a slaughterhouse, where the samples were extracted and immediately headed to the laboratory where the bioimpedance measurements were performed. The measured bioimpedance spectrum points contained 32 modulus and phase values at frequencies in the range from 500 Hz up to 1 MHz. A set of 20 pairs of reactance and resistance points corresponding to the lowest frequencies (from 500 Hz up to 60 kHz) was processed with a PSO algorithm.

#### 2.4.1.1 The PSO algorithm

PSO is inspired by bird flocking, where one may consider a group of birds that moves through the space searching for food, and that uses the birds nearer to the goal (food) as references (Xiaohui et al., 2004). PSO algorithms to fit a known function to experimental data is a technique similar to the one using genetic algorithms (GA). PSO has however a faster convergence for unconstrained problems with continuous variables such as the addressed fitting problem of the Cole-Cole function and has a simple arithmetic complexity (Hassan et al., 2005). Briefly, the PSO algorithm can be separated in the following steps:

1. Population initialization;

2. Evaluation of the particles in the population by a heuristic function, where in this case the particles are formed by a vector with the Cole-Cole function parameters;
3. Selection of the fittest particles (set of parameters) to lead the population towards the best set and
4. Update of the position and velocity of each particle by repeating the steps from 2 to 4 until a stopping condition is satisfied (Xiaohui et al., 2004).

Each parameter of the optimized function, in this case the fitting of the Cole-Cole function in eq. 5 to an experimental bioimpedance spectrum, can be represented as one dimension in the search space. The velocity update rule for the  $i$ -th particle is given by:

$$v_{id} = w \times v_{id} + c_1 \times rand() \times (p_{id} - x_{id}) + c_2 \times rand() \times (p_{nd} - x_{id}) \quad (6)$$

where  $v_{id}$  is the velocity of the  $i$ -th particle in the dimension  $d$ ;  $w$  is the inertia weight, in the  $[0, 1]$  range;  $c_1$  and  $c_2$  are the learning rates, usually in the  $[1, 3]$  range;  $rand()$  is a random number in the  $[0, 1]$  interval,  $p_{id}$  is the best position of the  $i$ -th particle for the  $d$ -th dimension and  $p_{nd}$  is the best neighborhood position for the  $d$ -th dimension. The particle position is updated by summing the present position to the velocity.

Each particle is made by a vector with the parameters  $[R_0, R_\infty, \tau_0, \alpha]$  of the Cole-Cole function, that are randomly initialized with arbitrary values in an interval corresponding to the physical limits of the system. A parameter restart step for the global search, inspired by the genetic algorithm mutation operator, was added to the code to prevent the premature convergence of the algorithm.

Like a genetic algorithm, the PSO enhances the solution based on a heuristic function, named fitness function, that measures the difference between the experimental spectrum and the fitted one. The fitness function is shown in eq. 7

$$fitness(p) = -\frac{1}{N} \sum_{i=1}^N abs(Z_i - A_i)^2 \quad (7)$$

It is defined by the modulus of the difference between the original complex bioimpedance experimental points,  $Z_i$ , and the fitted spectrum,  $A_i$ . As a consequence, resistance and reactance are taken into account in the function, and therefore, in the fitting.

#### 2.4.2 Artificial neural networks and the fitted functions of the bioimpedance spectrum

Artificial neural networks (ANN) were implemented such as to evaluate the behavior of the fitting algorithms to experimental data. This was developed to determine, comparatively, how much information the extracted parameters from the fitted Cole-Cole function may contain that represents correctly the experimental bioimpedances.

##### 2.4.2.1 ANN as used in BIA

One of the important features of a neural network resides in its capability to learn the relationships in a given data mapping, such as the mapping from the bioimpedance spectra to the type of the analyzed sample. This feature allows the network to be trained to perform estimations and classify new samples according to the learned pattern.

An ANN is composed of interconnected artificial neurons, each neuron being a simple computer unit (Haykin, 1999). Although a single neuron can perform only a simple operation, the network computational power is significant (Cybenko, 1989; Gorban, 1998) and can tackle any computable problem (Siegelmann & Sontag, 1991), under certain circumstances.

In a perceptron-like network such as the ones employed in this work, each neuron performs the operation shown in eq. 8, where  $y$  is the output value, defined as the result of the activation function  $\phi$  evaluated with the summation of  $m$  input signals  $x_i$ , each one multiplied by a weight  $w_i$  (also seen in fig. 4). All neural networks had neurons using the symmetric sigmoid activation function (Haykin, 1999). It is mathematically represented with its input in eq. 8. In eq. 9, the description of the sigmoid function is shown, and in fig. 3 a graphical illustration of its output is depicted as a function of its input for different steepness parameters. For this work, the steepness parameters were determined empirically. In the classification experiments, the parameter is  $s_{tp} = 0.65$  in the bovine flesh classification and  $s_{tp} = 0.5$  in the milk classification.

$$y = \phi \left( \sum_i^m x_i w_i \right) \tag{8}$$

$$\phi(x) = \frac{2}{1 + e^{-2s_{tp}x}} - 1 \tag{9}$$

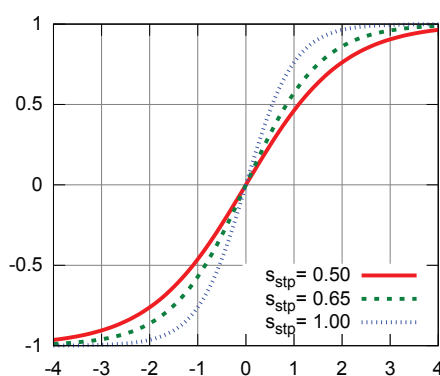


Fig. 3. Symmetric sigmoid function for distinct steepness  $s_{tp}$  values. In the experiments,  $s_{tp} = 0.65$  and  $s_{tp} = 0.5$ .

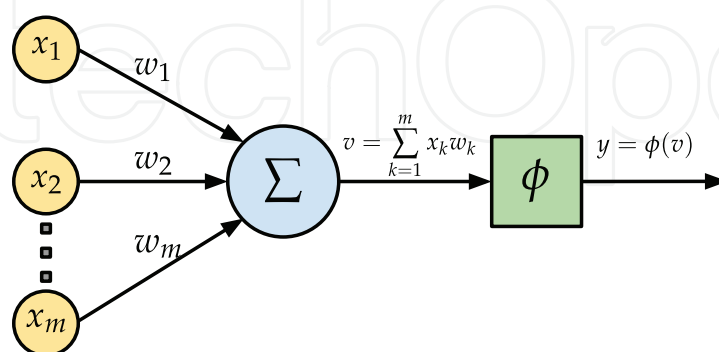


Fig. 4. Artificial neuron diagrammatic representation.

The ANN learns by adjusting its weights  $w_i$ . These weight changes are performed by using a training algorithm in the training stage (offline training), feeding the network with the input values and comparing the outputs with the expected result values, which would provide an

error measure. The calculated error is the information used to modify the weights of the connections, in order to reduce the errors on the next run. This procedure can be executed many times until the error converges to a minimum. The training procedure for the networks employed in this work are based on the following steps (error backpropagation procedure):

1. Feed the input data (Cole-Cole parameters or raw bioimpedance spectrum points) to the network;
2. Compute the output value of all neurons from the current layer and then propagate the results to the next layer (forward propagation);
3. Compare the network outputs at the output layer with the expected ones to have an error measure;
4. Propagate the measured errors to the previous layers, in a way that each neuron has a local error measure (back propagation);
5. Adjust the connection weights of the network, based on the local errors;

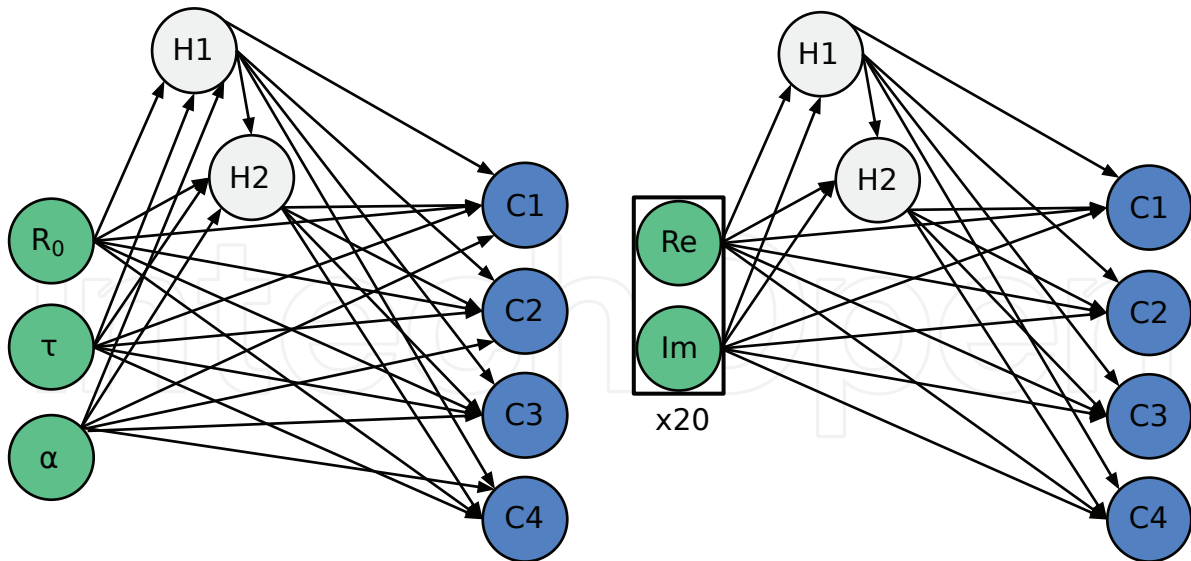
Different training algorithms can be used to adjust the weights of an ANN. It is common to supervised training algorithms to follow the same steps as the error backpropagation procedure, differing only in the weight adjusting step (Haykin, 1999). As an example, while the classical backpropagation has only a centralized learning rate, the iRPROP algorithm (Anastasiadis & Ph, 2003) has a learning rate for each connections and uses only the sign changes in the local error to guide the training. Other algorithms like NBN (Neuron by Neuron) uses the local errors to estimate second-order partial derivatives, which in some cases can lead to a faster training (Wilamowski, 2009).

In the bovine tissue classification experiment, two different fully connected cascade (FCC) topologies were employed. Both topologies had two hidden layers (with one neuron each) and an output layer with 4 neurons. The first one diagrammatically depicted in fig. 5(a) employed only 3 neurons in the input layer, for the  $R_0$ ,  $\tau$  and  $\alpha$  fitted Cole-Cole parameters, while the other one depicted in fig. 5(b) used 40 input neurons, corresponding to 20 impedance and reactance pairs. Both topologies had the goal of mapping the input data into one of 4 classes. To implement this, 4 output neurons were used, each one corresponding to a class. The NBN training algorithm was used to adjust the synaptic weights for the network to predict the correct beef classes.

The milk adulterant detection experiment employed a multilayer perceptron (MLP) topology (as in fig. 5(c)), with 30 input neurons (15 impedance and reactance pairs), one hidden layer with two neurons and an output layer with 3 neurons. Each output neuron corresponds to one class (one of C classes coding). The ANN was trained with the NBN algorithm.

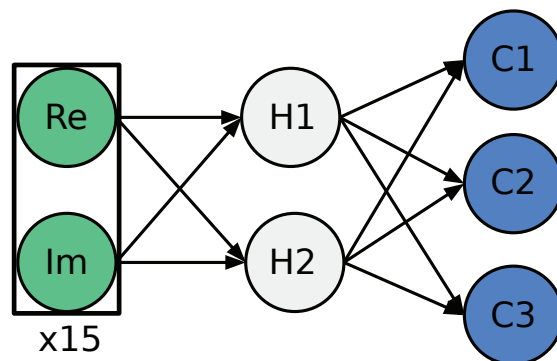
#### 2.4.2.2 Experiments with the ANN testing

The evaluated experimental data were also added to artificial noise such as to determine the robustness of the ANN classification when trained with the raw experimental points, with and without artificial noise, and also with the extracted parameters using different fitting techniques. Additionally, a genetic algorithm to similarly extract Cole-Cole function parameters (Halter et al., 2008) and the least-squares minimization algorithm for the fitting (Kun et al., 2003; 1999) were implemented to provide comparative results using the same methodology. It is expected that the stochastic algorithms may produce a set of parameters with small variances and with approximately the same mean values when



(a) 3–2–4 FCC topology employed in the bovine tissue classification experiment.

(b) 40–2–4 FCC topology employed in the bovine tissue classification experiment. The input layer has 40 neurons condensed in the box or 20 times 2 ('x20').



(c) 30–2–4 MLP topology employed in the milk adulterant detection experiment. The input layer has 30 neurons condensed in the box or 15 times 2 ('x15').

Fig. 5. Topology of artificial neural networks used in the experiment of bioimpedance spectra classification with bovine tissue and adulterated milk.

executed several times with the same set of experimental data. This would happen if the Cole-Cole function were an appropriate representation of the acquired bioimpedance spectrum data.

The resulting fitted parameters were used as input to the neural networks such as to classify the data by means of its known type (liver, heart, topside, or back muscle). Another neural network performed the same classification, but using the unprocessed spectrum points as inputs. The input signal was incrementally added to white-gaussian noise (AWGN) such as to produce different signal to noise ratios. A total of 24 electrical impedance measurements

were divided into two sets. The first set is formed by 15 measured spectra and is used for the neural network training, while the second set formed by the remaining 9 measurements were used for the neural network validation test. Another 11 sets were created with AWGN having signal-to-noise ratio (SNR) from 2 to 32 dB with steps of 2 dB, forming the base validation set where each spectrum was used more than once to sum a total of 20 spectra in each set. Four ANN were created, one for each fitting algorithm and another for the raw spectra. Each neural network was trained with the spectra from the training set and tested with the validation sets, using the corresponding results from the extracted Cole-Cole parameter output or the raw spectra as input. The neural networks for the use with the testing of fitting algorithms have a 3 – 2 – 4 fully connected cascade (FCC) topology to allow a better generalization in the ANN (Wilamowski, 2009), as diagrammatically illustrated in fig. 5, with the 3 input neurons corresponding to the  $[R_0, \tau_0, \alpha]$  parameters and the 4 output neurons corresponding to the confidence level of each bovine tissue type.

The neural network that uses the set of bioimpedance spectrum points as input with a 40 – 2 – 4 FCC topology had the 40 inputs corresponding to the real and imaginary parts of the 20 input spectrum points associated with the lowest frequencies in the experimental spectrum which would correspond to a maximum frequency of 60 kHz.

One ANN was trained with the parameters fitted by the PSO algorithm using the training set, by exposing the ANN to the sample values associated with the input that corresponds to the extracted Cole-Cole parameters. After that, the neural network performance was measured to classify the sample type correctly. The rate of correct classifications was calculated by using the extracted parameters and also the raw data from 11 spectrum and using the corresponding trained ANN.

### 2.4.3 Raw milk evaluation through bioimpedance spectra

In the dairy industry, conductivity measurements are made to test for abnormal milk. This is somehow similar to the process of obtaining a bioimpedance spectrum from a milk sample. However, in conductivity tests the sample is usually interrogated at a single frequency and the results give false positives and negatives (Belloque et al., 2008). Conductivity, therefore bioimpedance (Piton et al., 1988), and acidity measurements are also used to measure microbial contents of the milk, being indirect and rapid methods (Belloque et al., 2008; Hamann & Zeconi, 1998). The drawbacks of these methods are associated with the lack of sensitivity and specificity. In addition, the conductivity test is also included in screening tests to detect mastitis. Since mastitic milk contains pathogens and spoilage microorganisms, and it is also characterized by an increase in  $\text{Na}^+$  and  $\text{Cl}^-$  as well as leucocytes (Kitchen, 1981), this may be indicated by changes in bioimpedance spectrum (Bertemes-Filho, Negri & Paterno, 2010) as discussed here, and it would also characterize the analysis of raw milk as of a cell suspension.

Other changes in the milk, which may not have its causes in a sick animal, could also be indicated by changes in the bioimpedance spectrum, as when the milk has water or hydrogen peroxide, for example, added to it for fraudulent purposes (Bertemes-Filho et al., 2011). The modulus and phase of the bioimpedance along a frequency range containing more than one frequency point is therefore an extension of the typical measurement of conductivity in the process of milk quality evaluation and is justified by previous published results.

#### 2.4.3.1 Detection of water and hydrogen peroxide in raw milk

Milk may be adulterated by the addition of water, food coloring, conservants and substances used for the milk thickening, as for example the hydrogen peroxide. The commonest method of adulterating milk may be the dilution of water and a common method to detect it is by measuring its freezing point and use this value to calculate the percentage of the diluted water (Belloque et al., 2008). Another indication of water content would be provided by changes of bioimpedance spectra from the milk. To illustrate it, the bioimpedance spectra from raw milk with and without added water and hydrogen peroxide were determined and compared with each other.

An ANN is subsequently used to classify the milk sample by using the points of the bioimpedance spectrum. For this purpose, samples of raw milk from 27 Holstein cows in lactation were obtained in a local farm. The sample sets were divided into two groups. The first group (A) was used to train the neural network with 16 samples. From this set, 4 samples were randomly taken and had distilled water added to them in a volumetric concentration of 10%; other 4 samples had hydrogen peroxide added to them in a volumetric concentration of 3%. In the second group (B), 11 samples were used for the ANN validation, this is, to test if the trained algorithm correctly classifies the samples, that were also equivalently adulterated. Before the measurements, the samples were kept in a refrigerator at a temperature of 4°C for 4 hours.

The ANN used the multilayer perceptron topology of fig.5(c) with 30 neurons corresponding to resistance and reactance input values at 15 different frequency points in the bioimpedance spectrum. The output layer was formed by 3 neurons corresponding to a defined class (raw milk, milk with water and milk with hydrogen peroxide). If the bioimpedance spectrum of a sample containing H<sub>2</sub>O<sub>2</sub> is fed to the ANN, this output neuron must have the largest value output among the other two output neurons.

The ANN was trained using the Neuron by Neuron (NBN) algorithm by using 24 spectra, in which 4 samples were adulterated with water and other 4 with H<sub>2</sub>O<sub>2</sub>. For the ANN validation, 30 milk bioimpedance spectra were measured in a different data set producing another data set different from the one used in the training. The validation spectra were then separated into three different classes associated with the evaluated types of samples and the percentage of correct classifications were calculated.

#### 2.4.3.2 Evaluation of mastitic milk

The bioimpedance spectra of raw milk were acquired in samples from 17 Holstein cows, three of them with mastitis infection. Three milk samples of 100 ml from each animal were collected and stored in a refrigerator at a temperature of 4°C. Four hours later, the bioimpedance spectrum from each sample was collected and the material was sent to an accredited laboratory to characterize the presence of somatic cells and bacteria by using flow cytometry<sup>1</sup>. Selected samples had the acquired bioimpedance spectrum data points processed and the experimental points and Cole-Cole parameters analyzed and shown for illustration purposes of the changes presented in the mastitic and raw milk spectra.

<sup>1</sup> The laboratory managed to follow the International Dairy Federation Standards 148:2008 and 196:2004. These standards specify, respectively, methods for the counting of somatic cells and for the quantitative determination of bacteriological quality in raw milk.

### 3. Results and discussion

#### 3.1 Retrieving modulus from phase in experimental bioimpedance spectra

In the experiment to illustrate the effectiveness of modulus retrieval from the data acquired by the bioimpedance spectrometer, four vegetables were excited by a signal from the tetrapolar probe. Phase and modulus were acquired in the previously specified range at non-uniformly distributed frequencies. The first procedure in the experimental data was the interpolation to produce uniformly spaced points in the frequency range. The values of phase from the bioimpedance spectrum fed the algorithm to retrieve modulus. It is seen that the impedance at high frequencies is a small value tending to zero in one of the vegetables. However both data allowed the recovery of modulus from phase with an average error as shown in table 1 and as shown in fig. 6, where the behavior of the estimated modulus error is shown with the modulus from phase and the actual acquired phase for mango, banana, potato and guava. A higher error was observe in low frequencies since the lowest measured frequency was 500 Hz. In this experiment, the constraints for the use of the algorithm are such that it allowed the modulus recovery from the phase with a well-behaved error, and one can also infer that depending on the evaluated sample, the response of the algorithm may provide smaller errors.

As a general rule, the resistance at infinite frequencies must tend to zero for the algorithm to converge. In the case of an organic material suspension or a sample with a previously known bioimpedance and whose spectrum are not supposed to change much during its interrogation, the algorithm may be a convenient choice to substitute modulus measurements in bioimpedance interrogations while reading only phase. The resulting magnitude value associated with the modulus is normalized, since it is produced differently from the actual impedance value to a scale factor, requiring calibration.

Vegetable	Mean Error	Deviation $\sigma$
Mango	2.34%	2.84%
Banana	1.54%	2.86%
Potato	5.2%	6.06%
Guava	2.94%	1.96%

Table 1. Mean errors in modulus retrieval and standard deviation for the evaluated interval for mango, banana, potato and guava.

#### 3.2 PSO fitting using the Cole-Cole function in bovine flesh bioimpedance

Due to the noise incorporation characteristics (convergence to the mean noise level) caused by the presence of a constant value in the model function, the  $R_\infty$  parameter is neither included in the results, nor in the classification experiment. Since the signal-to-noise ratio (SNR) of the experimental data was changed by adding white gaussian noise to the experimental data points, this would be another reason not to include the  $R_\infty$  parameter in the performance tests. The  $R_0$  and  $\alpha$  parameters did not show any significant fluctuation differences when they resulted from any of the tested fitting algorithms, either the PSO or the Genetic Algorithm or the Least-Squares ordinary fitting, implemented as proposed in the literature (Halter et al., 2008; Kun et al., 2003; 1999). The results of the computational performance experiment depicted in table 2 contains both the mean and sample standard deviation of the required iterations for the convergence of the PSO algorithm and also for comparison purposes, the iterations needed for the convergence of the Genetic Algorithm and for the execution of the

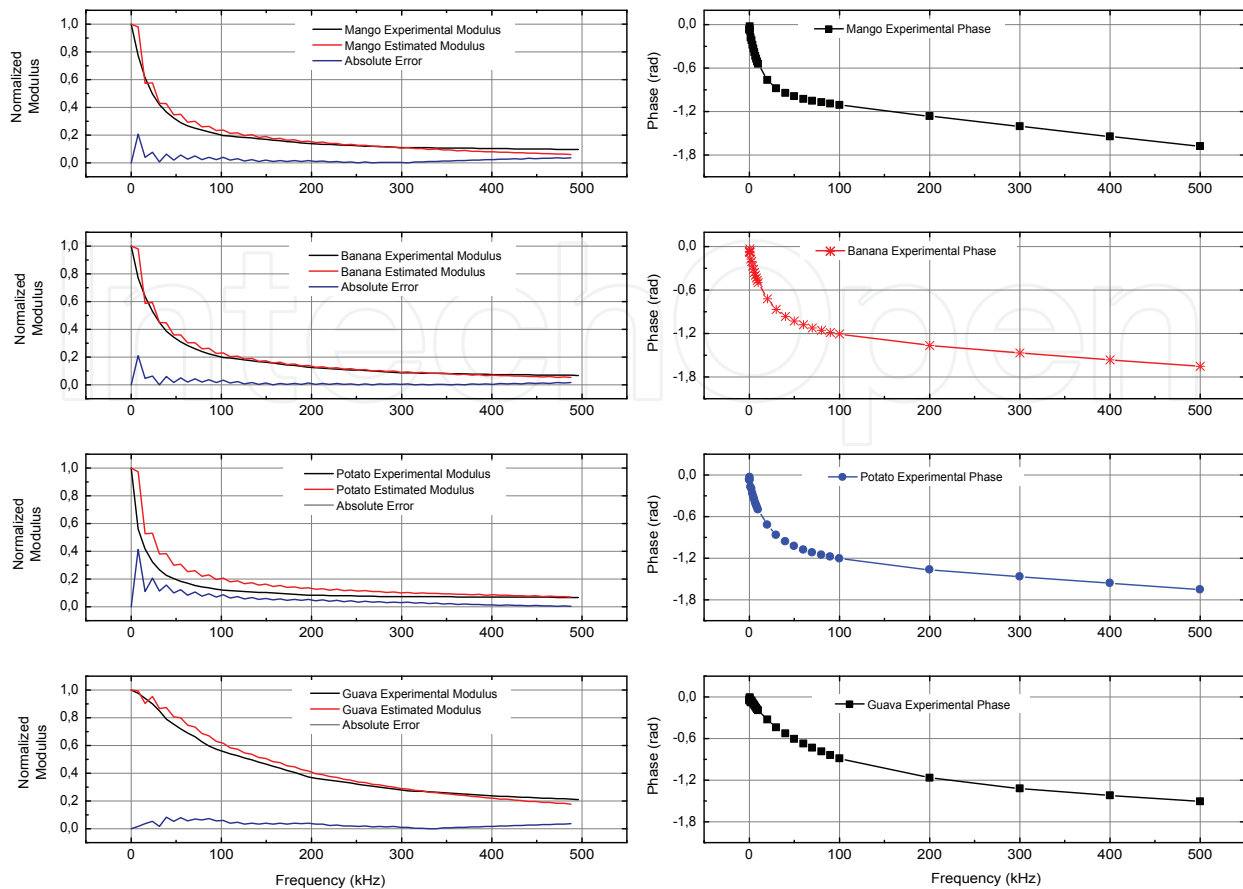


Fig. 6. Modulus retrieval obtained with the phase/modulus retrieval algorithm previously described. The input data was the interpolated 64 points of phase from the mango, banana, potato and guava.

Least-Squares (LS) fitting. Since the LS method is not stochastic, the deviation statistic is not applicable in this case. In fig. 7, the percentage of correct classification rate is depicted for the trained artificial neural networks using as inputs the parameter sets resulting from each of the fitting methods. The unprocessed bioimpedance spectrum points (raw) were used as inputs to an ANN with 40 input neurons, and the classification rate is also depicted in fig.7 together with the results from the testing of the PSO, LS and GA for an ANN with three input neurons.

Fitting Method	$\bar{n}$	$\sigma_n$
PSO	30	5.63
LS	134	Not applicable
GA	600	402.33

Table 2. Mean number of iterations,  $\bar{n}$ , for convergence of each fitting method producing a parameter set for the ANN input and its standard deviation for the stochastic fitting methods,  $\sigma_n$ .

From fig. 7, one may infer that the GA and proposed PSO methods demonstrate a higher accuracy and noise tolerance than the LS method, since under a higher SNR the used parameters provide the information for the correct classification of the samples. The LS method does not provide a better accuracy since for higher values of SNR, the experimental

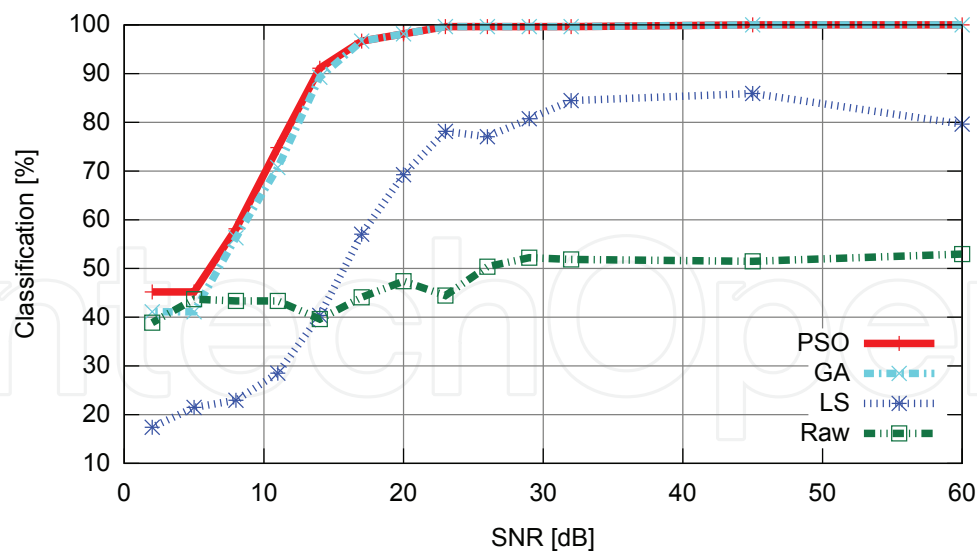


Fig. 7. Neural network classification rate when using as inputs the parameters from the fitting methods (PSO, GA and LS) and also the unprocessed bioimpedance spectrum points (Raw).

data still have distortions caused by artifacts or external effects in the system that may cause its parameters to provide a wrong guess in the classification. The Cole-Cole parameters with any fitting technique also produce improved results than when using a data set with the raw spectrum points in the classification. The quality of the LS fitting performance is influenced by its noise sensitivity. When tested with experimental points that have distortions from the electronic system or errors caused during the acquisition process from the material sample, the LS algorithm converged prematurely, producing parameter sets that deteriorated the classification. As the inputs provided by the PSO and GA methods produced a better classification rate and resulted in networks with reduced neurons and synaptic connections than using the full spectrum points, it is possible to recommend their use for bioimpedance classification systems even under worse SNR than usual.

In addition, the used model function was such that it was appropriate for the proposed methodology and allowed the verification of a conformity between the experimental bioimpedance spectrum and the Cole-Cole function to a certain degree, even with AWGN and other unavoidable artifacts. In the case of the experimental points without artificial AWGN added to the data, the results of the fitted spectra are depicted in fig. 8. In this case, it is also observed that the PSO/GA methods produce a better approximation to the experimental data, intrinsic distortion of the used BIA system notwithstanding.

It is equivalently shown in table 2, about the performance of the algorithms, that the PSO method converges faster, requiring less iterations than the GA method. The PSO algorithm also has a linear complexity per iteration with respect to the input data vector size. Due to implementation characteristics and its deterministic nature, the LS algorithm has the fastest performance, two orders of magnitude faster than what is obtained with the PSO and GA. It is possible to infer that the LS method has a superior computational performance than the other two fitting methods, and is followed respectively by the PSO and GA methods.

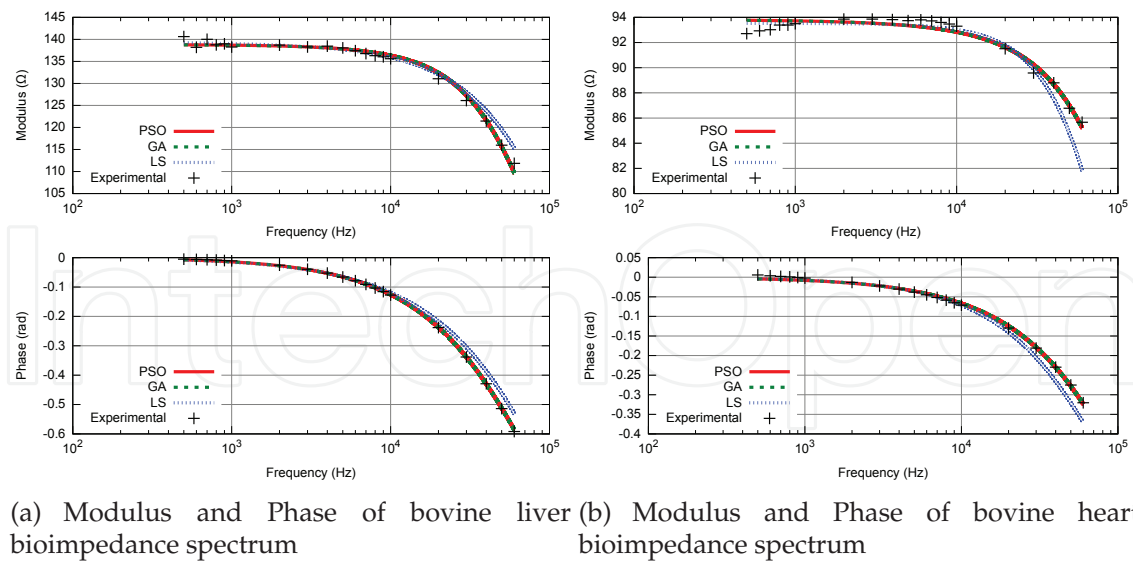


Fig. 8. Experimental data points containing modulus and phase of bioimpedance spectra of liver and heart samples from bovine flesh tissue. Experimental points are shown with the curves associated with the fitted Cole-Cole functions using PSO, LS and GA.

### 3.3 Abnormal milk testing with bioimpedance

#### 3.3.1 Spectra of adulterated milk

In fig. 9(a),(b) and (c), the bioimpedance spectra from the pure raw milk, and raw milk adulterated with water and hydrogen peroxide are depicted. The data were processed with the three fitting algorithms, and it is evidenced that the LS algorithm did not allow a proper fitting to the experimental points since one may observe a larger error along a wide frequency interval in the fitting. Since the PSO and GA have an equivalent qualitative performance, but a better computational performance in the PSO, the Cole-Cole parameters may represent more properly the information contained in the bioimpedance spectra. For higher frequencies, the Cole-Cole function is not capable of representing the experimental points characteristics in the phase spectrum, due to non-ideal characteristics and intrinsic artifacts and distortions inserted by the BIA system and the probe.

Comparatively one can observe some improvement in the fitting while using the PSO/GA algorithms in these data. However, distortions and artifacts produced by stray capacitance may cause a deviation in the resistance at high frequencies while obtaining the Cole-Cole parameters. Such changes may be observed in the complex impedance arc locus diagram plotted as the imaginary part of the bioimpedance as a function of its real part. The capacitive effect causes a hook like form in this diagram and the fitting process it may also produce a set of Cole-Cole parameters with negative resistances at high frequencies, as illustrated in fig. 9 (d).

In fig.10(a), the proportion of correct classification when using the raw data points to the trained ANN that classify adulterated milk is depicted and the average value of correct classifications is depicted as the total rate. It is observed that, if no other substance in the milk is related to the bioimpedance changes, except for the adulterants, the ANN is capable of properly characterizing the presence of water or hydrogen peroxide with a low error rate. The

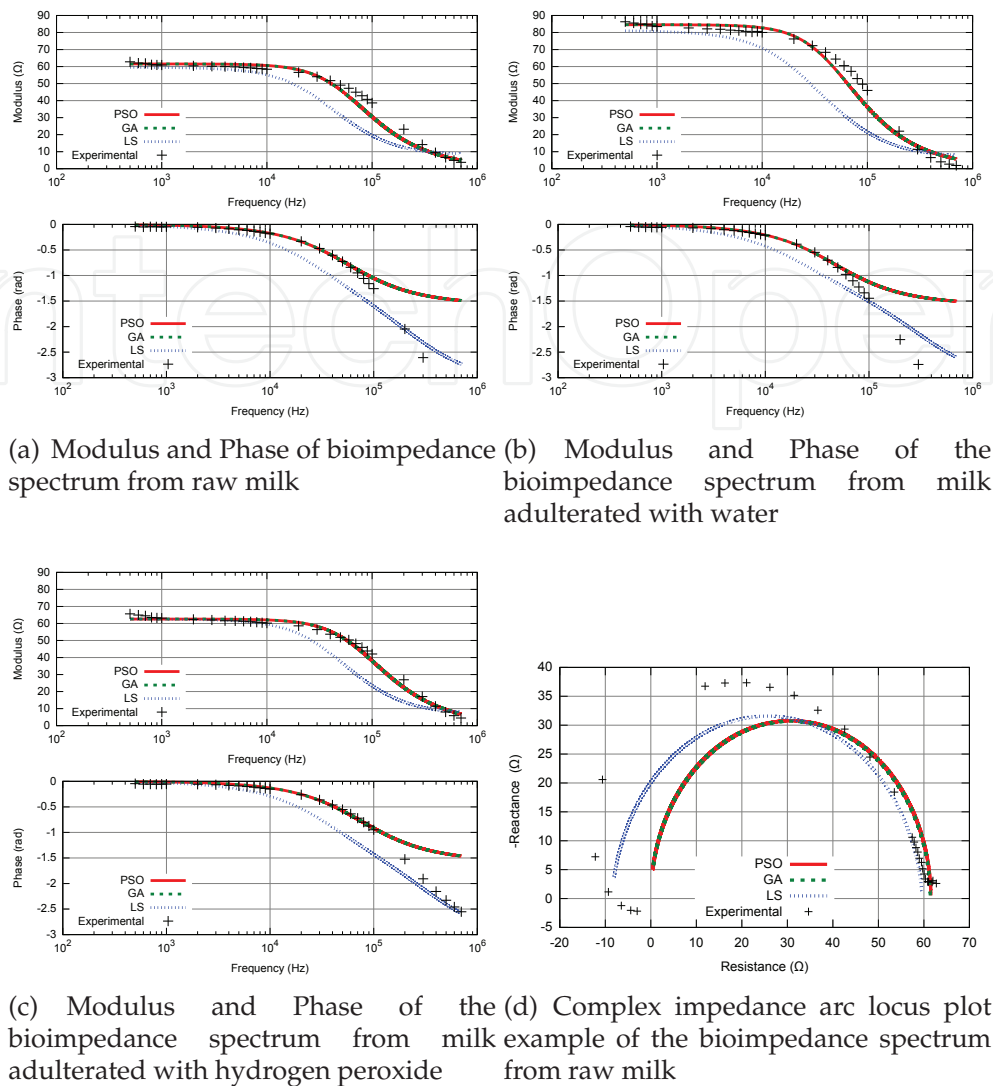


Fig. 9. Experimental bioimpedance spectrum and the results from the fitting with PSO, GA and LS algorithms. Data were obtained from raw milk and from raw milk adulterated with distilled water and with hydrogen peroxide. The complex impedance arc locus plot is depicted in fig. 9(d) associated with the raw milk sample.

used bioimpedance data have artifacts that were not corrected, and this was partly responsible for the non-null error in the classification rate.

In this evaluation of raw milk, it is possible to evidence the presence of artifacts that may invalidate the bioimpedance spectra. In order to avoid discarding spectra that may be corrupted mainly by impedance stray effects, usually the experimental data shown to have a hook-like form in the impedance plot at high frequencies requires that the data points be multiplied by a linear phase factor corresponding to a delay in the time domain. This would fit the experimental data with such distortions by multiplying the impedance function, i.e., an exponential factor  $e^{-j\omega T_d}$  (De Lorenzo et al., 1997). It would be equivalent to a delay of  $T_d$ s in the impedance time domain function if  $T_d$  is real and it would partly compensate the high frequency artifacts. The only problem in this compensation resides in the choice of the optimal  $T_d$  value, which is usually done on a trial-and-error basis.

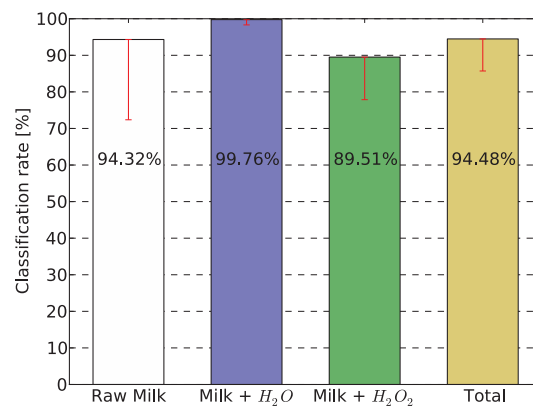


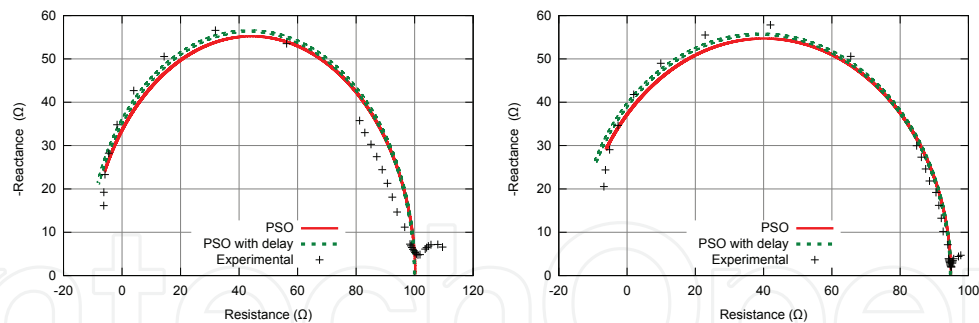
Fig. 10. ANN correct classification rate for adulterated milk when using raw spectrum points as inputs to the ANN.

### 3.3.2 Spectra of mastitic milk

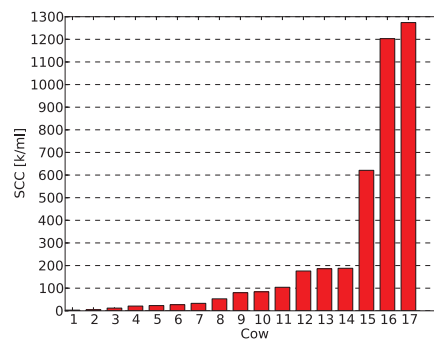
In the evaluation of the mastitic milk with different concentrations of cells, the graphs showing two examples of complex impedance arc locus are depicted in fig.11 (a) and (b). The somatic cell concentration (SCC) of the 17 milk samples as obtained from the accredited laboratory is shown in fig.11(c). The concentrations of 3000 cells per milliliter and 1.274 millions of cells per milliliter, as determined by the characterization in the laboratory, illustrate that the impedance spectra may confirm the differences between a mastitic milk sample with low cell concentration and mastitic milk. The impedance spectrum differences may be observed in the Cole-Cole parameters obtained in the fitting with the PSO technique while using also the compensation to reduce stray impedance effects, as depicted in fig. 11(a) and (b). The values of the fitting are depicted in table 3 for illustration purposes only and not to be used as references of mastitic milk bioimpedances. The compensation of stray impedance effects, however, may be used in any bioimpedance spectrum containing distortions due to stray impedances at high frequencies. The technique that shows how the optimal time delay for this compensation is obtained will be published elsewhere. The used  $T_d$ s are also shown in table 3 together with the mean squared error after the convergence of the algorithm and visually shows that the mean squared error between experimental points and fitted curves are reduced after correction. The resistances obtained by the model function fitting are also naturally reduced to zero, as observed in table 3. The parameters that change after time delay compensation may be

Parameters	Mastitic milk	Compensated mastitic milk	Raw milk	Compensated raw milk
$R_\infty$ [ $\Omega$ ]	-14.6	0	-11.7	0
$R_0$ [ $\Omega$ ]	94.9	94.8	100.3	100.7
$\alpha$	1	1	0.99	0.96
$\tau$ [ $\mu$ s]	0.552	0.515	0.711	0.672
$T_d$ [ $\mu$ s]	0	0.100726	0	0.110161
Mean Squared Error	14.6	9.2	31.6	26.9

Table 3. Cole-Cole parameters and final fitting mean squared error from the fitting with PSO algorithm for the spectra of mastitic milk samples and the bioimpedance from the raw milk sample, also containing the parameters from the fitted spectra compensated with specific time delays  $T_d$ .



(a) Complex impedance diagram of mastitic milk with 3000 cells per milliliter (b) Complex impedance diagram of mastitic milk with 1,274 millions of cells per milliliter



(c) Somatic cells concentration (SCC) for the 17 Holstein cows milk samples, given in thousands of cells per milliliter for each cow sample.

Fig. 11. The complex impedance arc locus diagram for two samples of milk with tolerable concentration of mastitis cells in fig. 11(a), a concentration above the limit characterizing mastitic milk in fig. 11(b). Experimental points and fitted curves with PSO and with the modified model function using the  $T_d$  parameter. In fig. 11(c), SCC for the evaluated samples.

markedly observed in the relaxation constant in the Cole-Cole function. The reciprocal of the relaxation constant would be related to the characteristic frequency of the sample that changes from 1.811 MHz to 1.941 MHz in the mastitic milk and in the compensated parameters. This indicates also that the experimental bioimpedance spectrum does not contain this frequency, requiring a wider frequency interval to evaluate more accurately the characteristics of the sample. In the low cell concentration mastitic milk, the parameters reflect a change in the frequency from 1.406 MHz to 1.488 MHz, that shows the same limitation in the experimental points, requiring a more detailed study where the spectrum will be analyzed with an analyzer in a wider frequency spectrum range.

In the results shown in table 4, the same compensation with a proper chosen time delay is applied to the Cole-Cole fitting and is compared to the parameters fitted with the PSO algorithm without compensation. One may observe that the low frequency resistance and the dispersion parameter  $\alpha$  is not affected by the compensation, but the compensated high frequency resistances are no longer negative. The improvement in the mean squared error of the final fitting procedure is significantly reduced, more than in the case of the compensation

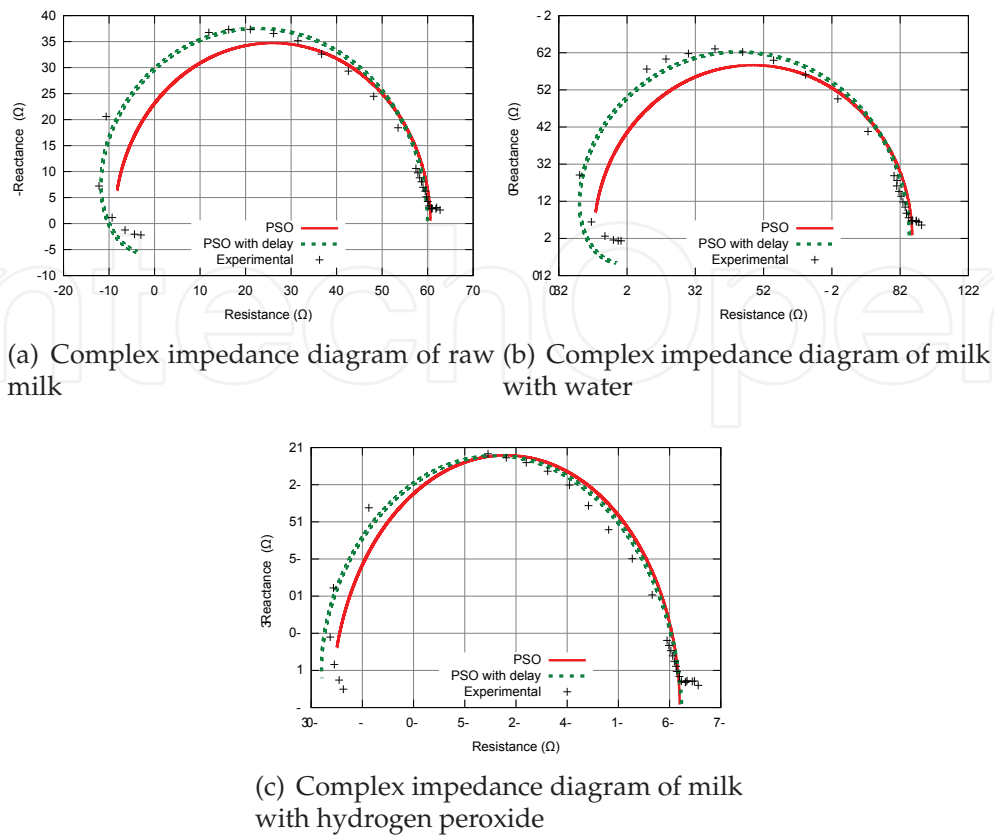


Fig. 12. The complex impedance arc locus diagram for samples of milk adulterated with water and hydrogen peroxide. The plots show the experimental points, the curve fitting with the Cole-Cole model function, and also the curve fitting containing the phase factor with the properly chosen time delay parameter.

Parameters	Raw milk	Compensated Raw Milk	Milk + H <sub>2</sub> O	Compensated Milk + H <sub>2</sub> O	Milk + H <sub>2</sub> O <sub>2</sub>	Compensated Milk + H <sub>2</sub> O <sub>2</sub>
$R_{\infty}$ [ $\Omega$ ]	-8.8	0	-9.7	0	-5.9	0
$R_0$ [ $\Omega$ ]	60.6	59.9	83.5	82.7	62	62.4
$\alpha$	1	1	1	1	1	0.95
$\tau$ [ $\mu$ s]	2.446	2.014	3.019	2.575	1.882	1.733
$T_d$ [ $\mu$ s]	0	0.595	0	0.631	0	0.301
Mean Squared Error	24	4.7	39.3	13.4	10.8	6.7

Table 4. Cole-Cole parameters and final fitting mean squared error from the fitting with PSO algorithm for the spectra of adulterated milk samples and the bioimpedance from a raw milk sample, also containing the parameters from the fitted spectra compensated with specific time delays  $T_d$ .

of the mastitic milk data. The complex impedance arc locus of the evaluated cases can be seen in fig. 12. It is evident from fig. 12 that the compensating time delay improves the fitting, indicating that the stray impedance effect is responsible for an important contribution to the

hook-like behavior of the complex impedance arc locus. Observing the dispersion parameter  $\alpha$ , it is usually close to unity in every sample, compensated or not. This is an indication that the milk may be modeled by a single pole function with fitting errors of the same order of magnitude as shown in table 4 and 3. Differently from the mastitic milk analysis, the reciprocal of the relaxation constant is in the experimental frequency interval obtained with the BIA system. The characteristic frequency of the samples in the raw milk changes from 408 kHz to 496 kHz after compensation. Equivalently for adulterated milk with water and hydrogen peroxide, the changes occur from 331 kHz to 388 kHz and from 531 kHz to 577 kHz, respectively. These variations indicate an increase in the compensated characteristic frequency when the stray effects are compensated this way.

#### 4. Conclusion

The authors report the use of computational intelligence and also well known digital signal processing algorithms in bioimpedance spectroscopy. The BIA analysis of data obtained from a custom made spectrometer were processed with a modulus retrieval algorithm from phase of bioimpedance spectra of vegetables showing the feasibility of using this specific and well known algorithm in a practical case. This would also allow the BIA system hardware to be simplified. In this case, since only the phase of the bioimpedance is going to be acquired to obtain the complete modulus of the bioimpedance spectrum, the involved electronic circuitry, as expected, may be reduced and the instrumentation amplifiers to measure modulus would be unnecessary. This would pave the way to embed algorithms in a much more simplified electronics for bioimpedance systems designed for specific applications as in the characterization of fruits, for example.

The bioimpedance data may also be processed with computational intelligence techniques. The authors improved already known techniques to fit experimental bioimpedance spectrum data to a specific model function. This is common practice in bioimpedance spectroscopy and is already implemented in commercial systems, however they do not use the techniques proposed here, only the least-squares algorithms, but no other more elaborate algorithms, like evolutionary techniques and particle-swarm optimization procedures. It is shown that the PSO technique has advantages over the already proposed procedures. The comparison of such techniques was implemented and artificial neural networks were used for the specific purpose of comparing them. The use of an Artificial Neural Network that receives as input the parameters produced by the fitting illustrates that different techniques, specifically the least-square fitting, simply would not be capable of allowing the identification of the correct tissue or the sample experimentally evaluated. The genetic algorithm and the particle-swarm optimization were capable of allowing the correct classification of the samples with experimental data added to noise in a much better proportion than the least-squares algorithm. Considering that the number of iterations in the PSO is much less than the genetic algorithm, and since they provide the same qualitative results in terms of classification, the PSO shows a superiority with respect to performance. The arithmetic complexity of the PSO is also an important characteristic that could facilitate embedded implementations.

Still in the dairy food applications, the idea of using bioimpedance to classify milk with the previously described techniques was also illustrated. Milk with different concentrations of mastitis cells were evaluated and the differences in the phase and modulus of the bioimpedance spectrum are noticed. However, the selectivity of the BIA system could not be demonstrated, and this would force one to use other additional sensing systems to

evidence the interesting characteristic. During the evaluation of adulterated milk with typical adulterants, like water and hydrogen peroxide, the information would be present in the bioimpedance spectrum, but an identification of the exact adulterant or its quantity would require other sensing systems.

The experimental data produced with the milk evaluation have also other characteristics not related to the sample itself, but to the instrumentation and also to reactions occurring between the sample and the electrode. The hook like figure in the complex plane arc locus in the milk measurements demonstrate the effect. Such a behavior may be considered due to adsorption in the impedance electrode in some types of samples. However, the hook-like characteristic of the spectrum may be due to impedance stray effects, either from the cables, electrodes or the electronic circuitry. This may be corrected in some cases with a change in the model, by considering the effect of a phase corresponding to a complex exponential in the model function. The optimal values were determined for the correction and the error in the fitting was significantly reduced in those sets of data. Specifically in the raw mastitic and adulterated milk, the Cole-Cole parameters were compared and the fitting algorithms are once again shown to be efficient in illustrating the computational power of the techniques in bioimpedance spectroscopy.

## 5. Future directions

The idea of determining efficient and simple algorithms to process bioimpedance spectra is a topic that may allow the implementation of sophisticated algorithms in embedded systems and could also improve the quality of the analysis produced by simple equipment. One can mention that in the case of the phase/modulus retrieval algorithms, since the technique is based on the use of the well-known fast-Fourier transform algorithm, it would be natural to implement it in embedded systems. However, the applications could not be restricted to such systems, since the use of the proposed algorithms may help improve the bioimpedance spectrum analysis while correcting experimental data and retrieving the more convenient information from the improved fitting algorithms. The methodology that uses artificial neural networks to evaluate the performance of the algorithms could also be used in systems that require automated analysis of bioimpedance spectra, as in an industrial environment to characterize samples of milk or beef, for example.

As a direction to the future research efforts, a final goal for the use of such algorithms would be their implementation in reconfigurable hardware, more specifically, in field-programmable gate arrays (FPGA). Commercial systems already use such technologies, like the FPGA in bioimpedance spectrometers (Nacke et al., 2011). Therefore the evaluated techniques are suggested to be implemented in hardware, since the particle swarm optimization algorithms would be a good choice for this purpose. The arithmetic operations in the particle-swarm optimization update step requires only random number generation, and a series of summations and multiplications. In the phase/modulus retrieval algorithm case, the FFT could also be easily instantiated from the core provided by the FPGA company.

## 6. Acknowledgements

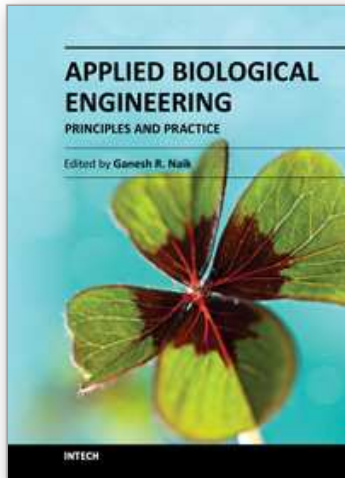
The authors gratefully acknowledge the experimental data collected by Rogerio Martins Pereira, Rodrigo Stiz and Guilherme Martignago Zilli as students supervised in the Laboratories of the Santa Catarina State University in Joinville City.

## 7. References

- Aberg, P., Nicander, I., Hansson, J., Geladi, P., Holmgren, U. & Ollmar, S. (2004). Skin cancer identification using multifrequency electrical impedance - a potential screening tool, *IEEE Transactions on Biomedical Engineering* 51(12): 2097–2102.
- Anastasiadis, A. D. & Ph, U. U. (2003). An efficient improvement of the RPROP algorithm, *In Proceedings of the First International Workshop on Artificial Neural Networks in Pattern Recognition*.
- Barsoukov, E. & Macdonald, J. R. (eds) (2005). *Impedance spectroscopy: theory, experiment and applications*, 2 edn, Wiley, New York.
- Belloque, J., Chicon, R. & Recio, I. (2008). *Milk Processing and Quality Management*, 1 edn, Wiley-Blackwell, West Sussex, United Kingdom.
- Bertemes-Filho, P. (2002). *Tissue Characterisation using an Impedance Spectroscopy Probe*, PhD Thesis, The University of Sheffield, UK.
- Bertemes-Filho, P., Negri, L. H. & Paterno, A. S. (2010). Mastitis characterization of bovine milk using electrical impedance spectroscopy, *Congresso Brasileiro de Engenharia Biomédica (CBEB) – Biomedical Engineering Brazilian Congress*, pp. 1351–1353.
- Bertemes-Filho, P., Negri, L. & Paterno, A. (2011). Detection of bovine milk adulterants using bioimpedance measurements and artificial neural network, in Ákos Jobbágy (ed.), *5th European Conference of the International Federation for Medical and Biological Engineering*, Vol. 37 of *IFMBE Proceedings*, Springer, pp. 1275–1278.
- Bertemes-Filho, P., Paterno, A. S. & Pereira, R. M. (2009). Multichannel bipolar current source used in electrical impedance spectroscopy: Preliminary results, in O. Dössel, W. C. Schlegel & R. Magjarevic (eds), *World Congress on Medical Physics and Biomedical Engineering, September 7 - 12, 2009, Munich, Germany*, Vol. 25/7 of *IFMBE Proceedings*, Springer Berlin Heidelberg, pp. 657–660.  
URL: [http://dx.doi.org/10.1007/978-3-642-03885-3\\_182](http://dx.doi.org/10.1007/978-3-642-03885-3_182)
- Bertemes-Filho, P., Valichski, R., Pereira, R. M. & Paterno, A. S. (2010). Bioelectrical impedance analysis for bovine milk: Preliminary results, *Journal of Physics: Conference Series* 224(1): 012133.  
URL: <http://stacks.iop.org/1742-6596/224/i=1/a=012133>
- Brown, B. H. (2003). Electrical impedance tomography (EIE): a review, *J. Med. Eng. Technol.* 3: 97–108.
- Cole, K. S. (1940). Permeability and impermeability of cell membranes for ions, *Cold Spring Harb. Symp. Quant. Biol.* 8: 110.
- Cole, K. S. (1968). *Membranes, Ions and Impulses: A Chapter of Classical Biophysics*, Biophysics Series, first edn, University of California Press.
- Cole, K. S. & Cole, R. H. (1941). Dispersion and Absorption in Dielectrics I. Alternating Current Characteristics, *The Journal of Chemical Physics* 9(4): 341–351.  
URL: <http://link.aip.org/link/doi/10.1063/1.1750906>
- Cybenko, G. (1989). Approximation by superpositions of a sigmoidal function, *Mathematics of Control, Signals, and Systems (MCSS)* 2: 303–314.
- De Lorenzo, A., Andreoli, A., Matthie, J. & Withers, P. (1997). Predicting body cell mass with bioimpedance by using theoretical methods: a technological review, *Journal of Applied Physiology* 82(5): 1542–1558. URL: <http://jap.physiology.org/content/82/5/1542.abstract>
- Fuoss, R. M. & Kirkwood, J. G. (1941). Electrical properties of solids. viii. dipole moments in polyvinyl chloride-diphenyl systems\*, *Journal of the American Chemical Society* 63(2): 385–394. URL: <http://pubs.acs.org/doi/abs/10.1021/ja01847a013>

- Gorban, A. (1998). Approximation of continuous functions of several variables by an arbitrary nonlinear continuous function of one variable, linear functions, and their superpositions, *Applied Mathematics Letters* 11(3): 45 – 49.  
URL: <http://www.sciencedirect.com/science/article/pii/S0893965998000329>
- Grimnes, S. & Martinsen, O. G. (2008). *Bioimpedance & Bioelectricity BASICS*, 2 edn, Academic Press.
- Halter, R. J., Hartov, A., Paulsen, K. D., Schned, A. & Heaney, J. (2008). Genetic and least squares algorithms for estimating spectral eis parameters of prostatic tissues, *Physiological Measurement* 29(6): S111.  
URL: <http://stacks.iop.org/0967-3334/29/i=6/a=S10>
- Hamann, J. & Zecconi, A. (1998). Bulletin 334, *Evaluation of the Electrical Conductivity of Milk as a Mastitis Indicator*, International Dairy Federation, pp. 1–23.
- Hassan, R., Cohanin, B., Weck, O. D. & Venter, G. (2005). A comparison of particle swarm optimization and the genetic algorithm, *46th AIAA/ASME/ASCE/AHS/ASC Structures, Structural Dynamics, and Materials Conference*, pp. 1–13.
- Hayes, M., Lin, J. S. & Oppenheim, A. V. (1980). Signal Reconstruction from Phase or Magnitude, *IEEE Transactions on Acoustics, Speech and Signal Processing* 28(6): 672–680.  
URL: <http://dx.doi.org/10.1109/TASSP.1980.1163463>
- Haykin, S. (1999). *Neural Networks*, Prentice-Hall, New Jersey.
- Holder, D. S. (2004). *Electrical impedance tomography: methods, history and applications*, 1st edn, Taylor and Francis, New York.
- Kitchen, B. J. (1981). Bovine mastitis: milk compositional changes and related diagnostic tests, *Journal of Dairy Research* 48(01): 167–188.  
URL: <http://dx.doi.org/10.1017/S0022029900021580>
- Kronig, R. D. L. (1929). The theory of dispersion of x-rays, *Journal of the Optical Society of America* 12(6): 547.  
URL: <http://dx.doi.org/10.1364/JOSA.12.000547>
- Kun, S., Ristić, B., Peura, R. A. & Dunn, R. M. (2003). Algorithm for tissue ischemia estimation based on electrical impedance spectroscopy, *IEEE Transactions on Biomedical Engineering* 50(12): 1352–9.
- Kun, S., Ristic, B., Peura, R. & Dunn, R. (1999). Real-time extraction of tissue impedance model parameters for electrical impedance spectrometer, *Medical and Biological Engineering and Computing* 37: 428–432.  
URL: <http://dx.doi.org/10.1007/BF02513325>
- Kyle, U. G., Bosaeus, I., Lorenzo, A. D. D., Deurenberg, P., Elia, M., Gómez, J. M., Heitmann, B. L., Kent-Smith, L., Melchior, J.-C., Pirlich, M., Scharfetter, H., Schols, A. M. & Pichard, C. (2004). Bioelectrical impedance analysis: part i. Review of principles and methods, *Clinical Nutrition* 23(5): 1226.
- Nacke, T., Barthel, A., Beckmann, D., Pliquett, U., Friedrich, J., Peyerl, P., Helbig, M. & Sachs, J. (2011). Messsystem für die impedanzspektroskopische breitband-prozessmesstechnik – broadband impedance spectrometer for process instrumentation, *Technisches Messen* 78(1): 3–14.  
URL: <http://www.olderbourg-link.com/doi/abs/10.1524/teme.2011.0077>
- Negri, L. H., Bertemes-Filho, P. & Paterno, A. S. (2010). Extração dos parâmetros da função de Cole-Cole utilizando otimização por enxame de partículas, *XXII Congresso Brasileiro de Engenharia Biomédica (CBEB) – Biomedical Engineering Brazilian Congress*, pp. 928–931.

- Nordbotten, B. J., Tronstad, C., Ørjan G Martinsen & Grimnes, S. (2011). Evaluation of algorithms for calculating bioimpedance phase angle values from measured whole-body impedance modulus, *Physiological Measurement* 32(7): 755.  
URL: <http://stacks.iop.org/0967-3334/32/i=7/a=S03>
- Paterno, A. S. & Hoffmann, M. (2008). Reconstrução de sinais em espectroscopia de bioimpedância elétrica, *XXI Congresso Brasileiro de Engenharia Biomédica (CBEB) – Biomedical Engineering Brazilian Congress*, pp. 1–4.
- Paterno, A., Stiz, R. & Bertemes-Filho, P. (2009). Frequency-domain reconstruction of signals in electrical bioimpedance spectroscopy, *Medical and Biological Engineering and Computing* 47: 1093–1102.  
URL: <http://dx.doi.org/10.1007/s11517-009-0533-1>
- Piton, C., Dasen, A. & Bardoux, I. (1988). Evaluation de la mesure d'impédance comme technique rapide d'appréciation de la qualité bactériologique du lait cru, *Lait* 68(4): 467–484.  
URL: <http://dx.doi.org/10.1051/lait:1988430>
- Proakis, J. G. & Manolakis, D. K. (2006). *Digital Signal Processing*, 4 edn, Prentice Hall.
- Quartieri, T. & Oppenheim, A. V. (1981). Iterative techniques for minimum phase signal reconstruction from phase or magnitude, *IEEE Transactions on Acoustics, Speech and Signal Processing* 29(6): 1187–1193.  
URL: <http://dx.doi.org/10.1109/TASSP.1981.1163714>
- Riu, P. J. & Lapaz, C. (1999). Practical limits of the Kramers-Kronig relationships applied to experimental bioimpedance data, *Annals of the New York Academy of Sciences* 873(1): 374–380.  
URL: <http://dx.doi.org/10.1111/j.1749-6632.1999.tb09486.x>
- Sieglmann, H. T. & Sontag, E. D. (1991). Turing computability with neural nets, *Applied Mathematics Letters* 4(6): 77 – 80.  
URL: <http://www.sciencedirect.com/science/article/pii/089396599190080F>
- Stiz, R. A., Bertemes, P., Ramos, A. & Vincence, V. C. (2009). Wide band Howland bipolar current source using AGC amplifier, *IEEE Latin America Transactions* 7(5): 514–518.
- Waterworth, A. R. (2000). *Data Analysis Techniques of Measured Biological Impedance*, Phd Thesis, The University of Sheffield, UK.
- Wilamowski, B. M. (2009). Neural network architectures and learning algorithms, *IEEE Industrial Electronics Magazine* 3: 56–63.
- Xiaohui, H., Yuhui, S. & Eberhart, R. (2004). *Congress on Evolutionary Computation, 2004 – CEC2004*, Vol. 1, IEEE, pp. 90–97.  
URL: [http://ieeexplore.ieee.org/xpl/freeabs\\_all.jsp?arnumber=1330842](http://ieeexplore.ieee.org/xpl/freeabs_all.jsp?arnumber=1330842)



## **Applied Biological Engineering - Principles and Practice**

Edited by Dr. Ganesh R. Naik

ISBN 978-953-51-0412-4

Hard cover, 662 pages

**Publisher** InTech

**Published online** 23, March, 2012

**Published in print edition** March, 2012

Biological engineering is a field of engineering in which the emphasis is on life and life-sustaining systems. Biological engineering is an emerging discipline that encompasses engineering theory and practice connected to and derived from the science of biology. The most important trend in biological engineering is the dynamic range of scales at which biotechnology is now able to integrate with biological processes. An explosion in micro/nanoscale technology is allowing the manufacture of nanoparticles for drug delivery into cells, miniaturized implantable microsensors for medical diagnostics, and micro-engineered robots for on-board tissue repairs. This book aims to provide an updated overview of the recent developments in biological engineering from diverse aspects and various applications in clinical and experimental research.

### **How to reference**

In order to correctly reference this scholarly work, feel free to copy and paste the following:

Aleksander Paterno, Lucas Hermann Negri and Pedro Bertemes-Filho (2012). Efficient Computational Techniques in Bioimpedance Spectroscopy, Applied Biological Engineering - Principles and Practice, Dr. Ganesh R. Naik (Ed.), ISBN: 978-953-51-0412-4, InTech, Available from:

<http://www.intechopen.com/books/applied-biological-engineering-principles-and-practice/efficient-computational-techniques-in-bioimpedance-spectroscopy>

**INTECH**  
open science | open minds

### **InTech Europe**

University Campus STeP Ri  
Slavka Krautzeka 83/A  
51000 Rijeka, Croatia  
Phone: +385 (51) 770 447  
Fax: +385 (51) 686 166  
[www.intechopen.com](http://www.intechopen.com)

### **InTech China**

Unit 405, Office Block, Hotel Equatorial Shanghai  
No.65, Yan An Road (West), Shanghai, 200040, China  
中国上海市延安西路65号上海国际贵都大饭店办公楼405单元  
Phone: +86-21-62489820  
Fax: +86-21-62489821

© 2012 The Author(s). Licensee IntechOpen. This is an open access article distributed under the terms of the [Creative Commons Attribution 3.0 License](#), which permits unrestricted use, distribution, and reproduction in any medium, provided the original work is properly cited.

IntechOpen

IntechOpen